Laboratory and Field Observations of an Apparent Sub-Capillary-Equilibrium Water Saturation Distribution in a Tight Gas Sand Reservoir*

K.E. Newsham[1] and J.A. Rushing[2]

[1]SPE, Anadarko Petroleum Corporation; currently Apache Corporation, Houston, Texas (kent.newsham@apachecorp.com)
[2]SPE, Anadarko Petroleum Corporation

Abstract

This article documents laboratory and field observations of an apparent sub-capillary-equilibrium water saturation distribution in the Bossier tight gas sands. These observations are validated with consistent measurements from several different techniques, including production performance analysis, reservoir fluid phase behavior, log evaluation, and both conventional and special core analyses. We also identify several mechanisms, including those associated with a basin-centered gas system, which may be responsible for this phenomenon.

Introduction

Tight gas sands constitute a significant percentage of the U.S. natural gas resource base and offer tremendous potential for future reserve growth and production. A recent study by the Gas Technology Institute (Prouty, 2001) indicated tight gas sands comprise almost 70% of gas production from all unconventional gas resources and account for 19% of the total gas production from both conventional and unconventional sources in the U.S. The same study (Prouty, (2001) estimated total producible tight gas sand resources exceed 600 tcf, while economically recoverable reserves are 185 tcf. This article focuses on one of the most active domestic U.S. tight gas sand plays, the Bossier Sands in the East Texas Basin. Specifically, we present results from a reservoir description and characterization study in the Mimms Creek and Dew fields in Freestone County, Texas.

Similar to conventional oil and gas systems, tight gas sands are often described by complex geological and petrophysical systems as well as heterogeneities at all scales. Unlike conventional reservoirs, however, tight gas sands often exhibit unique gas storage and producing characteristics.

Consequently, effective exploitation of these resources requires accurate description of key reservoir parameters, particularly water saturation. This article presents results of a Bossier tight gas sand characterization study from which capillary pressure data indicated a very high connate water saturation distribution throughout the entire vertical column. Yet, these low-permeability Bossier sands produce at economically viable rates even though relative permeability measurements suggest these rates are not possible unless the initial water saturation is lower than that predicted by capillary equilibrium. We attribute this anomalous production behavior to the presence of a sub-capillary-equilibrium distribution of water saturation; i.e., an unusually low water saturation distribution that cannot be predicted by conventional capillary pressure analysis.

We present laboratory and field observations of the Bossier sands, a deep abnormally pressured, high-temperature tight gas sand reservoir exhibiting an apparent sub-capillary-equilibrium water saturation distribution. These observations are based upon consistent measurements obtained from several different techniques, including production performance analysis, reservoir fluid phase behavior, log evaluation, and both conventional and special core analyses. We provide a detailed description of the analysis techniques used in our study and discuss specific results which indicate an unusually low water saturation distribution. We also identify several mechanisms, including those associated with a basin-centered gas system, which may be responsible for the long-term desiccation or evaporation of the connate water saturation.

Regional Geology and Depositional Environment

The Bossier sands are Late Jurassic in age and were deposited in the East Texas Basin. Located in northeast Texas, this sedimentary basin is a deep elongated trough structure with shelf-slope systems on the basin flanks. Several major tectonic features, including the Sabine Uplift to the east, the Mexia-Talco Fault System to the north and west, and the Angelina-Caldwell Flexure to the south bound the basin (Montgomery, 2000). East Texas is recognized as one of three major salt provinces in the U.S. The East Texas Basin is characterized by major salt features - salt anticlines, piercement domes, pillows, etc. within its interior (Montgomery, 2000). Current geological models suggest a relationship between generation of the major fault systems, salt deformation and migration, basin subsidence, and sediment deposition during Middle to Late Mesozoic (Montgomery, 2000). The significant salt structures also appear to control the distribution of sediments within the basin interior (Montgomery, 2000).

A typical stratigraphic column for the East Texas Basin (Figure 1) shows that the Bossier sands are part of the Upper Jurassic Cotton Valley Group and are overlain by the Cotton Valley Sandstone (Montgomery, 2000). The Bossier interval is thick and lithologically complex and contains black to gray-black shale interbedded with very fine- to fine-grained argillaceous sandstone. Similarly, the Cotton Valley Sandstones are comprised of interbedded shale and very quartz rich sandstone layers. The Cotton Valley Group is underlain regionally by the Upper Jurassic Louark Group. This includes other hydrocarbon-bearing formations such as the Smackover carbonates and Haynesville/Cotton Valley Limestones. Overlying the Cotton Valley Group is the regionally productive, Lower Cretaceous Travis Peak and Pettit (Sligo) formations.

As illustrated by the generalized regional dip-section in Figure 2, Bossier deposition represents cycles of sand progradation into the basin onto organic rich mud, succeeded by marine transgression. Much of the Bossier interval downdip appears to be time equivalent to the Cotton Valley Sandstone updip and represents prodelta/delta front material related to Cotton Valley deltaic systems (Montgomery, 2000; Perrizela, 2002). The Bossier sands appear to originate from the north and west and were transported downslope by slumping, debris flow, and turbidity currents. Significant Bossier sand thicknesses are located in topographic lows created by a combination of faulting, subsidence, and salt movement in the basin.
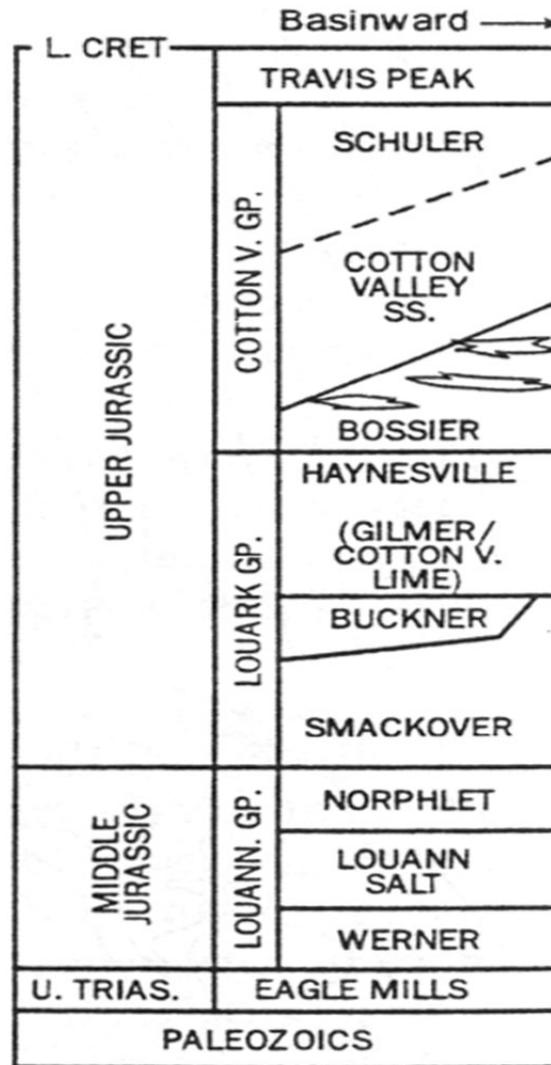
Figure 1. East Texas stratigraphic section. The Bossier sands are of Jurassic age found in the Lower Cotton Valley Group.
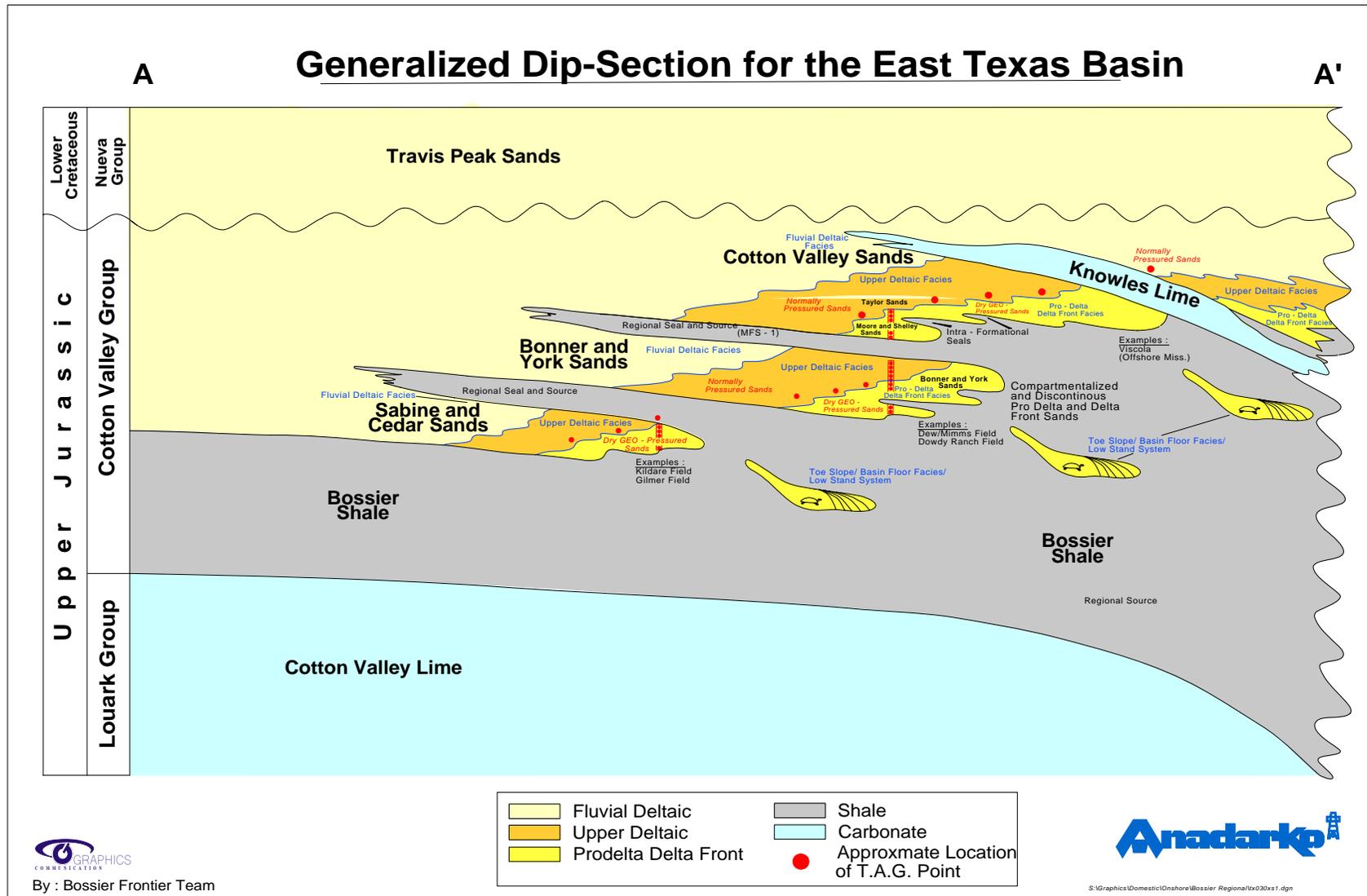
Figure 2. Generalized regional dip section of the Bossier facies. Sand deposition represents cycles of sand progradation into the basin onto organic-rich mud, succeeded by marine transgression. Much of the Bossier shales downdip appear to be time equivalent to the updip Cotton Valley Sandstone and represent prodelta/delta-front material related to Cotton Valley deltaic systems (drawing courtesy of Anadarko Petroleum Corporation, 1999).
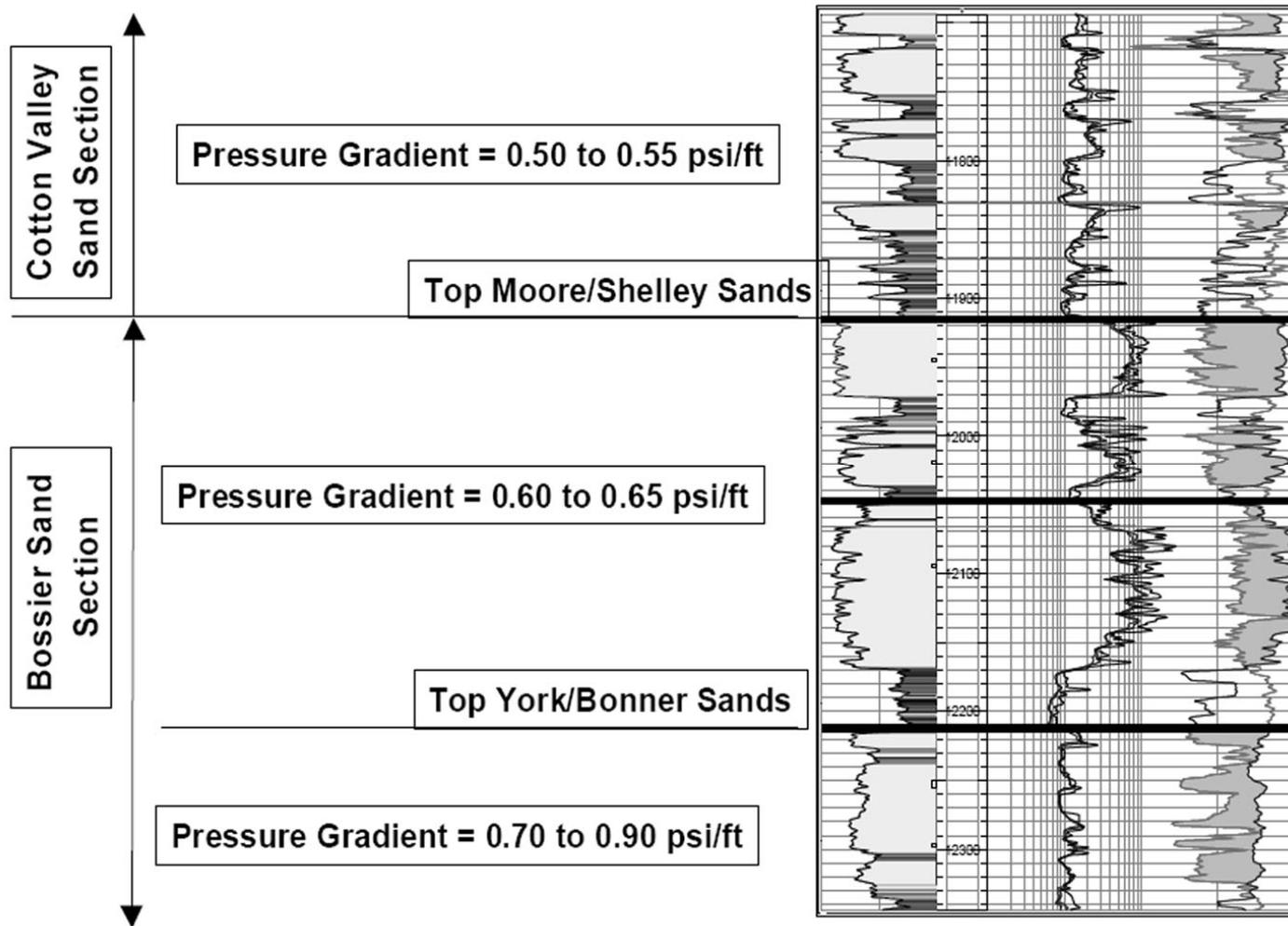
Figure 3. Type log of the Bossier Sands showing the range of observed pressure gradients and the sequence of sand deposition.

Bossier Sand Characteristics of the Mimms Creek and Dew Fields

The current Bossier sand play is centered along the western shelf margin of the East Texas Basin, specifically in Robertson, Leon, Limestone, and Freestone counties. In this section we summarize the reservoir characteristics of the Mimms Creek and Dew fields located in Freestone County. Much of the reservoir description is based on more than 1000 ft of whole core and more than 200 rotary sidewall core samples.

Sand Facies and Depositional Environment

The Bossier sands in Mimms Creek and Dew fields are comprised of a series of stacked sandy packages, as illustrated by the type log in Figure 3. In chronological order of deposition, these packages are known as the York, Bonner, Shelley, and Moore sands. Stratigraphic sequences observed from several whole cores indicate the sands were deposited as a prograding sediment wedge complex during a lowstand onto organic shelf mud deposited during a highstand. At the top of the sand packages, ravinement or transgressive lag deposits have been observed, indicating the onset of a marine transgression during which very little sand was preserved above wave base. The Bossier sands are capped by restricted to open shelfal muds deposited during another highstand (Perrizela, 2002).

As illustrated in Figure 4, typical Bossier sand-body geometry is elongated with the long axis oriented parallel to the depositional dip; so lateral continuity along depositional strike is often limited. The sand-body thickness varies from tens to several hundred feet. The combination of low depositional relief and limited lateral sand continuity minimizes the hydrocarbon column height potential within each sand body. In addition, the elongated geometry of the isolated sand bodies combined with low permeability and high degree of heterogeneity limits the volume of recoverable gas from a single well. This observation is confirmed from production decline type curve analysis

which indicates small drainage areas, typically ranging from 40 to 80 acres but frequently less than 40 acres per well.

Bossier Shale Characteristics

The Bossier shales are prevalent both areally and vertically in Mimms Creek and Dew fields. Laterally extensive shales appear to act as both seals and hydrocarbon source rock for the sands, while local interbedded shales also appear to be an important hydrocarbon source for the Bossier sands. A reservoir study of these shales shows current total organic carbon (TOC) ranges from 1% to 5%, while the kerogen type is mixed Type II and III. Vitrinite reflectance measurements average 1.25% but range from 1.2 to as high as 2.5%, indicating the shales are in the gas window for hydrocarbon generation. Measurements using the RockEval technique (Espitalie et al.., 1985) validated observations from the vitrinite reflectance data.

As we discuss in the next section, most of the Bossier section in the Mimms Creek and Dew fields is abnormally overpressured. A probable source for this overpressured system is gas generation from the shales. The data suggests hydrocarbons have been generated not only from kerogen cracking in the shales but also from cracking of liquid hydrocarbons trapped in the sands. This cracking phenomenon, which has been documented by Hunt (1990), has been postulated on the basis of pyrobitumen observed in core thin sections. We also conducted gas isotope analysis on Bossier gas samples, and the

computed carbon isotope separations (δ^{13}C) range from –30 ppt to –40 ppt which is consistent with gases of thermal origin. Gases produced from the Mimms Creek and Dew fields are composed primarily of methane, but we also measure ethane and small quantities of propane, which are also indicative of thermal rather than biogenic origin.

Pressure and Temperature Gradients

The Bossier Sands are overpressured throughout most of the East Texas Basin, including the Mimms Creek and Dew Field area. As illustrated by Figure 3, pressure gradients range from 0.50 to 0.55 psi/ft in the upper Cotton Valley Sands, 0.60 to 0.65 psi/ft in the upper Bossier, Moore, and Shelley Sands, and 0.70 to 0.90 psi/ft in the lower Bossier Bonner and York Sands. The Cotton Valley Sand pressure gradient represents a normal to slightly abnormal pressure gradient of a very saline formation water column (>220,000 ppm NaCl). A pressure transition exists throughout the Bossier interval with the pressure gradient increasing with depth in a basinward direction.

This overpressured system, which has been confirmed using both static bottomhole pressure measurements and from acoustic log analysis (Figure 5), is easily recognized by pressure-depth profiles. The deviation from the normal pressure gradient is referred to as the top of abnormal pressure (TAG) point. The overpressure gradient, when calculated from mean sea level, increases with depth; however, the pressure transition trend, referred to as the incremental pressure gradient (IPG), ranges from 3.5 psi/ft to 5.00 psi/ft. Note that the IPG is significantly greater than the lithostatic gradient. The inequality between the lithostatic and incremental pressure gradients suggests the source of overpressure is not caused by compaction/disequilibrium (Swarbrick and Osborne, 1998; Finkbeiner, 2001). Rather, we believe the source of overpressure is primarily from hydrocarbon generation and secondarily from chemical compaction effects of diagenesis.

Bossier sands in this area and throughout the East Texas Basin also exhibit abnormally high temperature gradients. Bottomhole temperatures in the Mimms Creek and Dew fields range from 280°F to 325°F at depths ranging from 12,500 ft to 13,500 ft. This corresponds to temperature gradients of 2.2 to 2.4^{o}F per 100 ft of depth.

Typical Producing Characteristics

The average initial gas production rates vary from 2 to 5 MMscfd in the Moore and Shelley sands, while the Bonner and York sands range from 5 to 15 MMscfd. Similarly, the estimated ultimate gas recovery ranges from 1.5 to 3 Bcf in the Moore and Shelley sands and 3 to 10 Bcf in the Bonner and

York. Most wells exhibit hyperbolic decline with stabilized rates of 500 to 900 Mscfd after two to three years. The differences between producing characteristics in the sands reflect both better reservoir quality and higher pressures in the Bonner and York sands.

The Bossier sands also produce some water. Initial water production rates, which range from 50 to 100 bbl/d for the first one to three months, can be attributed to clean-up of stimulation fluids. However, most wells produce between 1 to 5 bbl/day for the life of the well. Because of the low permeability of the Bossier sands, we do not believe a mobile liquid phase exists in the reservoir. The source of long-term water production is probably

condensed water vapor. This observation seems to be confirmed by the low salinity of the produced waters.

Fluid Properties

Wells completed in the Bossier sands produce a dry to slightly wet gas, with specific gravity ranging from 0.58 to 0.61. Condensate production averages one to three STB/MMscf over the life of the well. Gas composition typically averages 94 mole% methane and 2 mole% ethane.

The remaining hydrocarbon mixture includes fractional percentages of propane through hexane, with typically no heptanes plus. Non-hydrocarbon components include 2 to 2.5 mole% carbon dioxide, 0.2 to 0.5 mole% nitrogen, and relatively no hydrogen sulfide.

As we noted above, the Bossier sands produce some water; however, we believe that no mobile liquid water phase exists in the reservoir. Laboratory analyses indicate that five to ten mole% of water vapor may be dissolved in the gas at reservoir conditions. Consequently, most of the low water production rate over a well's life can be attributed to condensed water vapor.

Intrinsic Rock Properties

We have also conducted a comprehensive Bossier sand description program, using evaluations of more than 1000 ft of whole core obtained from four wells in the Mimms Creek and Dew fields. Our description includes classification of petrophysical rock types, which are identified based on similar pore and grain scale characteristics, such as composition, texture, mineralogy, clay type, and types of diagenesis. We have also defined several hydraulic rock types representing similar ranges of storage and flow characteristics. Table 1 summarizes the various measurements made to describe the Bossier sands.

Petrographic Rock Types

The petrographic rock types observed within the Bossier Sands (Newsham and Rushing, 2001) include clean sandstone, argillaceous/weakly laminated sandstone, dolomitic sandstone, and argillaceous/burrowed siltstone (Newsham and Rushing, 2001). Using the Folk (1974) classification, the types range from subarkose to sublitharentite to lithic wackes. The framework grains contain, on average, 84% quartz, 6.5% feldspar, and 9.5% rock fragments. The range for these constituents is 41%-94% for quartz, 0%-11.7% for feldspar, and 0.5%-59% for the rock fragments.

The intergranular constituents are primarily quartz overgrowths, diagenetic clay in the sands, detrital clay found in sand and silt, dolomite cement, and local pyrite. The clay fraction is dominantly grain-coating chlorite and illite. Texturally, the Bossier Sands have a narrow range of grain size, typically from upper very fine to fine. The sands are medium to well sorted, while the silts are typically poorly sorted. Sand grain shape is subangular to well rounded. A significant degree of compaction is observed from thin sections in the form of suturing, elongation of grain contacts, and ductile grain deformation.

Bossier sands also exhibit a significant diagenetic overprint. Diagenesis, the physical or chemical processes that cause changes in the initial rock

properties, tends to modify the initial pore structure and geometry. This results in an increase in the tortuosity from a reduction in pore throat size and a subsequent increase in the number of isolated and disconnected pores. Most diagenetic effects are

manifested as reductions in permeability and porosity. The most important forms of diagenesis in the Bossier sands are mechanical compaction, cementation from quartz overgrowths, grain-coating/pore lining clay development, and grain dissolution. Although less important and prevalent, carbonate cementation has also been observed in Bossier sandstones.

Hydraulic Rock Types

We have also identified several Bossier sand hydraulic rock types (Newsham and Rushing, 2001). When described on the basis of the dominant pore throat diameter determined from high-pressure mercury capillary pressure data, we observed distinct groupings of rocks having similar flow and storage properties; i.e., hydraulic rock types. Figure 6 is an example of an incremental mercury intrusion plot used to identify rock types (Pittman, 1992; Gunter et al., 1997; Washburn, 1921; Swanson, 1979; Thompson et al., 1987; Newsham and Rusing, 2001). Figure 7 shows the general region of each rock type in porosity-permeability space, while Table 2 lists the permeability, pore throat aperture size, and range of initial water saturation conditions. Hydraulic rock types 1, 2A, 2B, and 3A are all considered as reservoir rock. Because of their low permeability, high initial water saturation and significant degree of vertical heterogeneity, rock types 3B and 4 are non-reservoir rocks and probably act as flow baffles, barriers, and seals.

Effective Porosity and Absolute Permeability

Figure 7 shows a typical distribution of effective porosity and absolute permeability. Effective porosity varies from 1% to 17%, while absolute permeability ranges from 0.001 to 1 mD. Non-reservoir and seal rocks have permeability values lower than 0.001 mD. In general, the Bonner and York sands have better permeability and porosity than the Moore and Shelley sands. Better reservoir quality combined with higher pressures is demonstrated by greater gas recovery.

Similar to most tight gas sands, the Bossier sands display both stress-dependent porosity and permeability characteristics. For example, the hyperbolic decline behavior exhibited by many tight gas sand wells can be attributed, in part, to reductions in permeability and porosity during the depletion history. We measured porosity and permeability over a wide range of stress conditions and observed slight changes in porosity. We did, however, measure significant reductions in permeability as net mean stress is increased. We also noticed that the degree of stress dependency increased for the lower quality rock types.

Effective and Relative Permeability

Although we believe no mobile liquid phase exists in the Bossier sands at reservoir conditions, the presence of water does affect gas flow capacity. Consequently, we measured effective gas permeability for a range of water saturation. Figure 8 shows computed relative permeability curves for hydraulic rock types 1, 2A and 2B. All of the curves were normalized to 5% initial water saturation based on the minimum water saturation measured

in rock type 1. Note that, for the entire range of hydraulic rock types, the effective permeability to gas is reduced significantly for water saturation greater than 40% to 60%.

Water Saturation

We also measured connate water saturation from more than 500 Bossier whole core plugs. Since the whole core was obtained with a low invasion, oil-base mud system, we were able to obtain consistent and accurate estimates of in-situ connate water saturation. We used the Dean Stark solvent extraction technique with toluene as the solvent. Most of the non-reservoir rock had water saturation greatly exceeding 60%. Measured water saturation in the reservoir rock, however, ranged from 5% in hydraulic rock type 1 to 50% in hydraulic rock type 3A. These measured water saturations, especially in the best reservoir rock, were significantly lower than we expected. Consequently, we sought to verify these values with log-based calculations and capillary pressure characteristics.

Capillary Pressure Characteristics

We measured capillary pressure characteristics using high-pressure, mercury injection (MICP). We used MICP since the low porosity and permeability precluded using either centrifuge or porous plate methods, which are limited by the maximum attainable pressure. From the capillary pressure measurements, we were able to describe the vertical water saturation distribution (Leverett, 1041; Gunter, 1999; Negabahn et al., 2000), range of irreducible water saturation, and capillary seal capacity. As noted above, we also identified hydraulic rock types using capillary pressure characteristics.
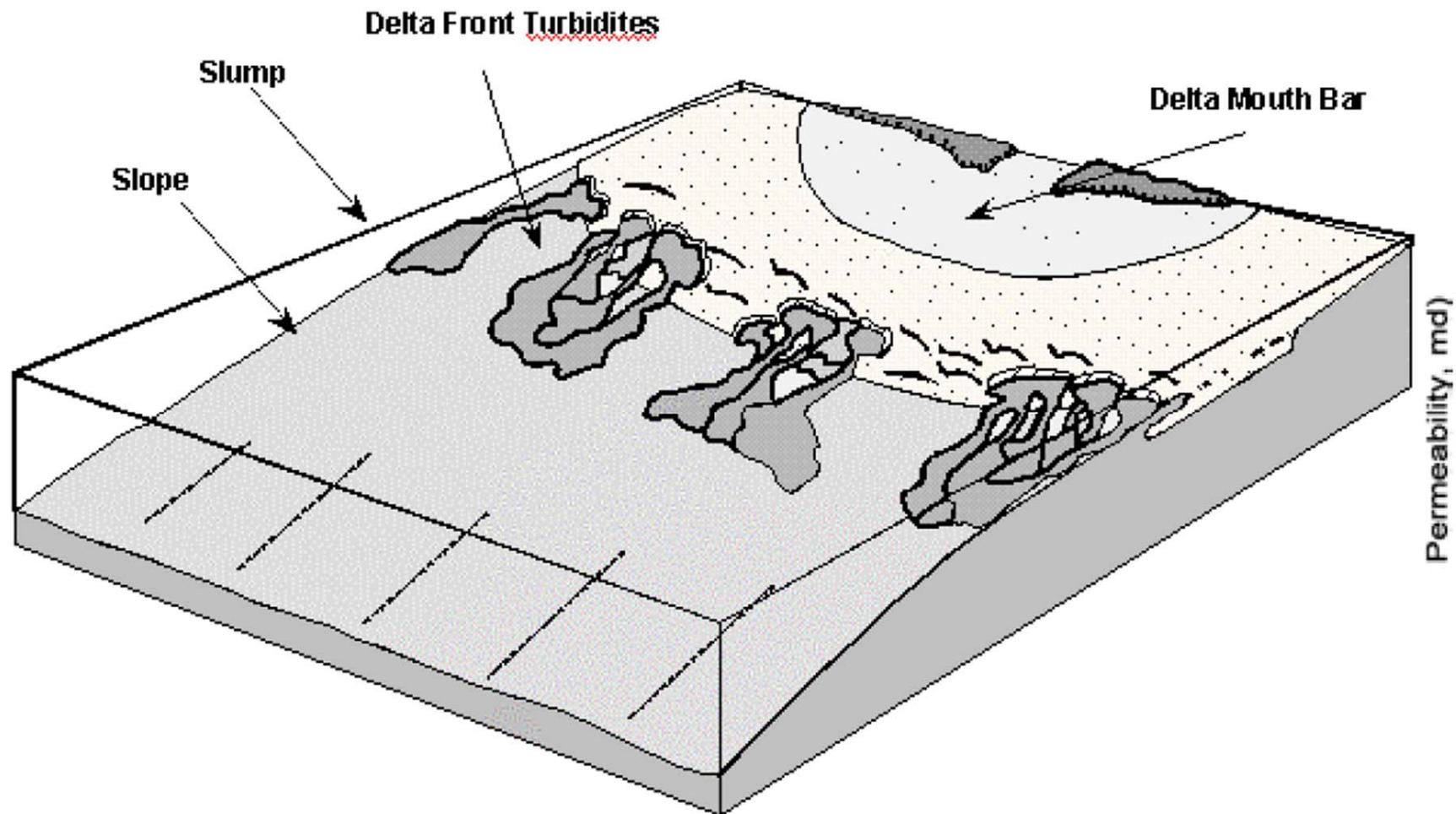
Figure 4. Typical Bossier sand body geometry is elongated and oriented with the long axis parallel to the depositional dip. Lateral sand continuity along depositional strike is often limited, resulting in sands with small dimensions and limited continuity. The sand body thickness varies from tens to several hundred feet.
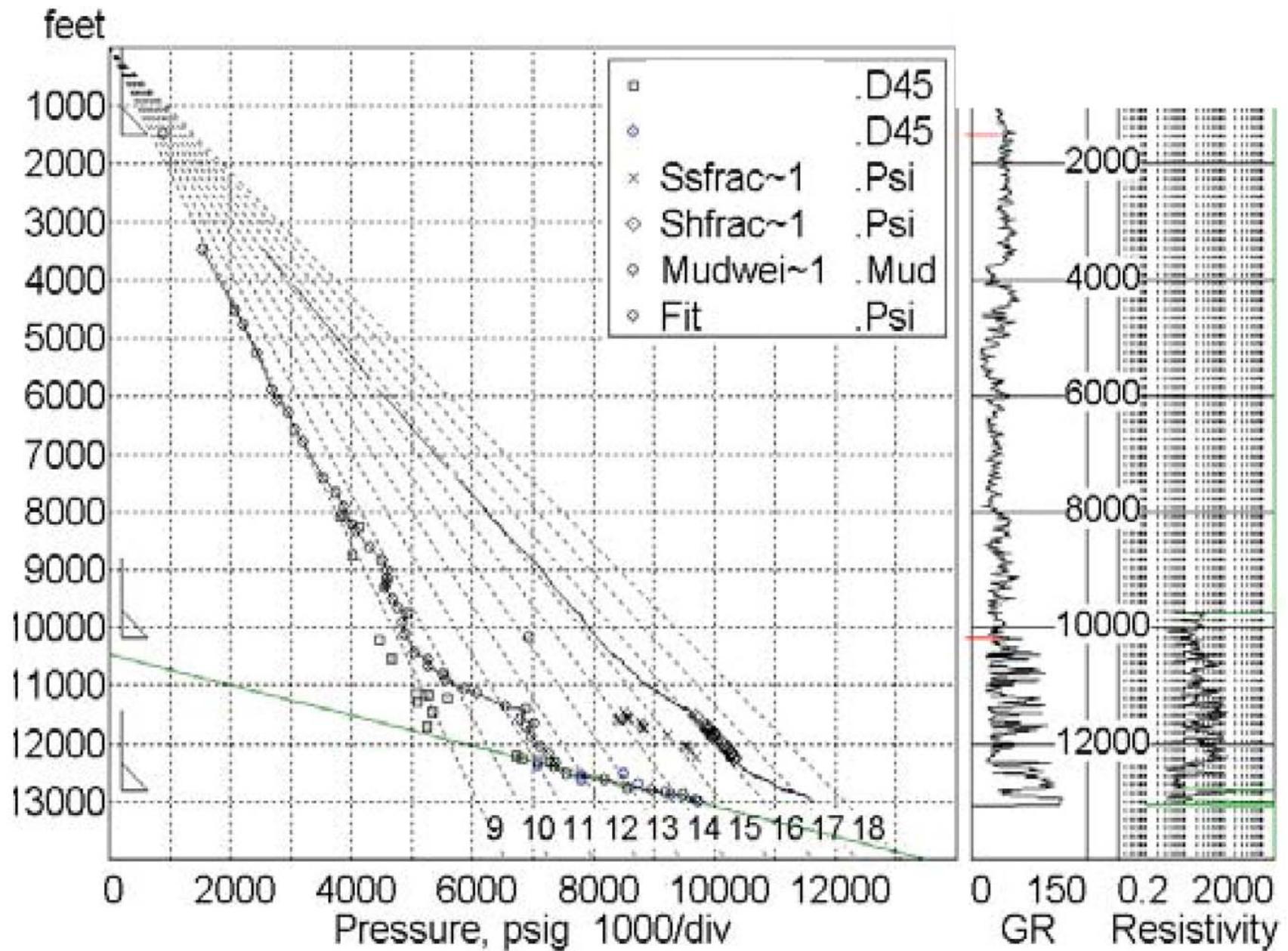
Figure 5. An example of a typical vertical pressure distribution estimated from the acoustic log response.
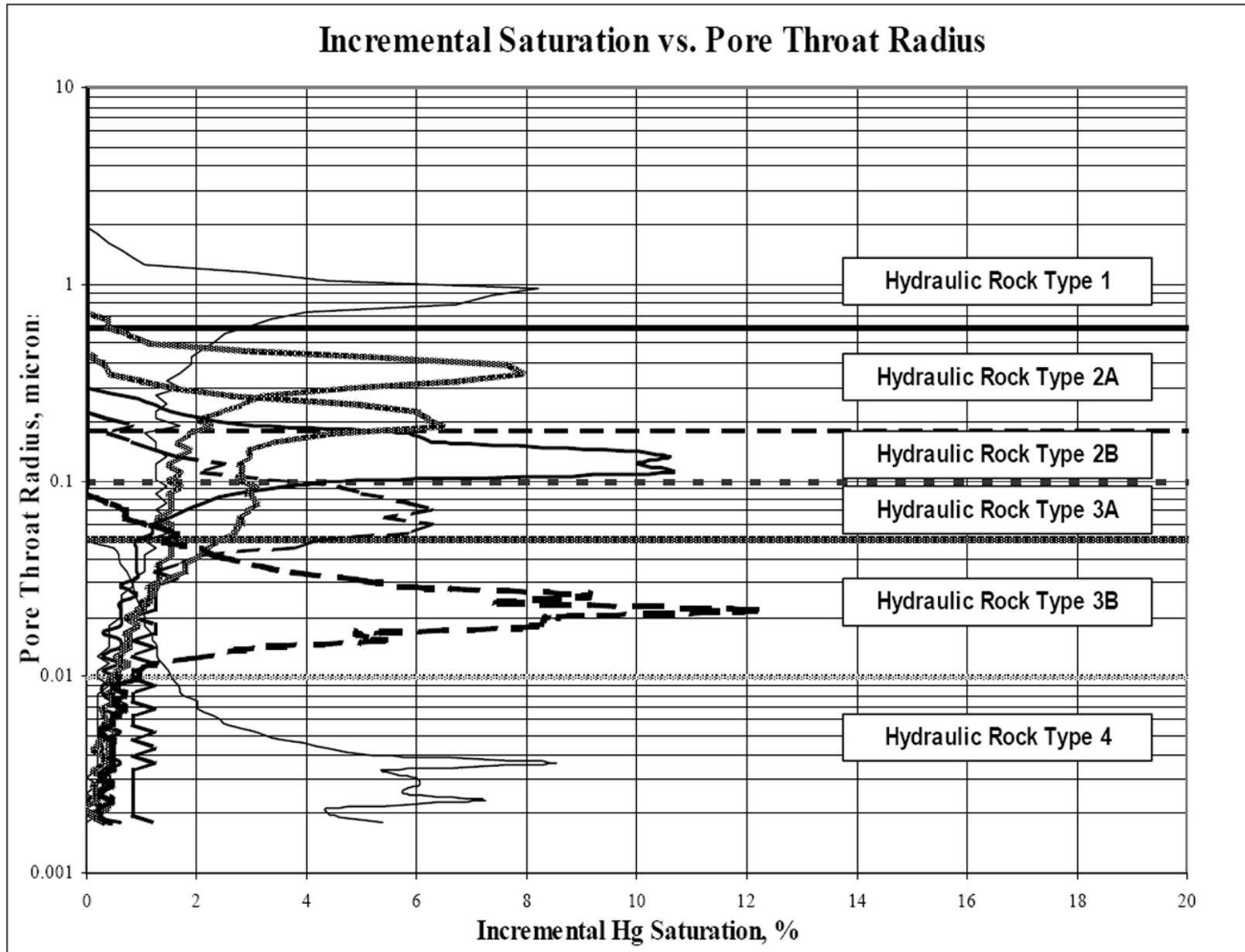
Figure 6. Incremental mercury intrusion plot used to identify hydraulic rock types for the Bossier sands.
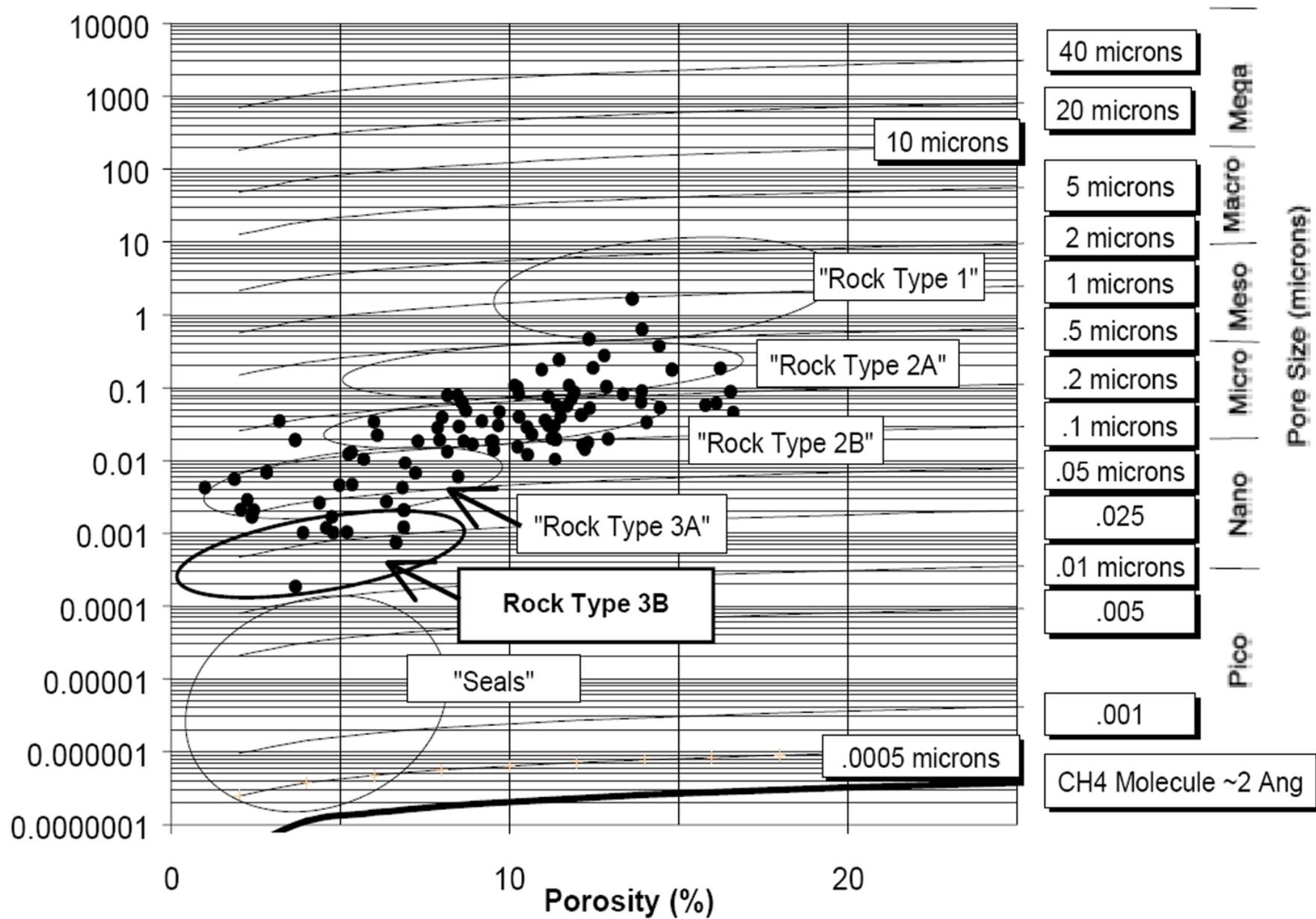
Figure 7. Porosity and permeability plot showing the general region of each rock type (ovals) for the Bossier Sand.
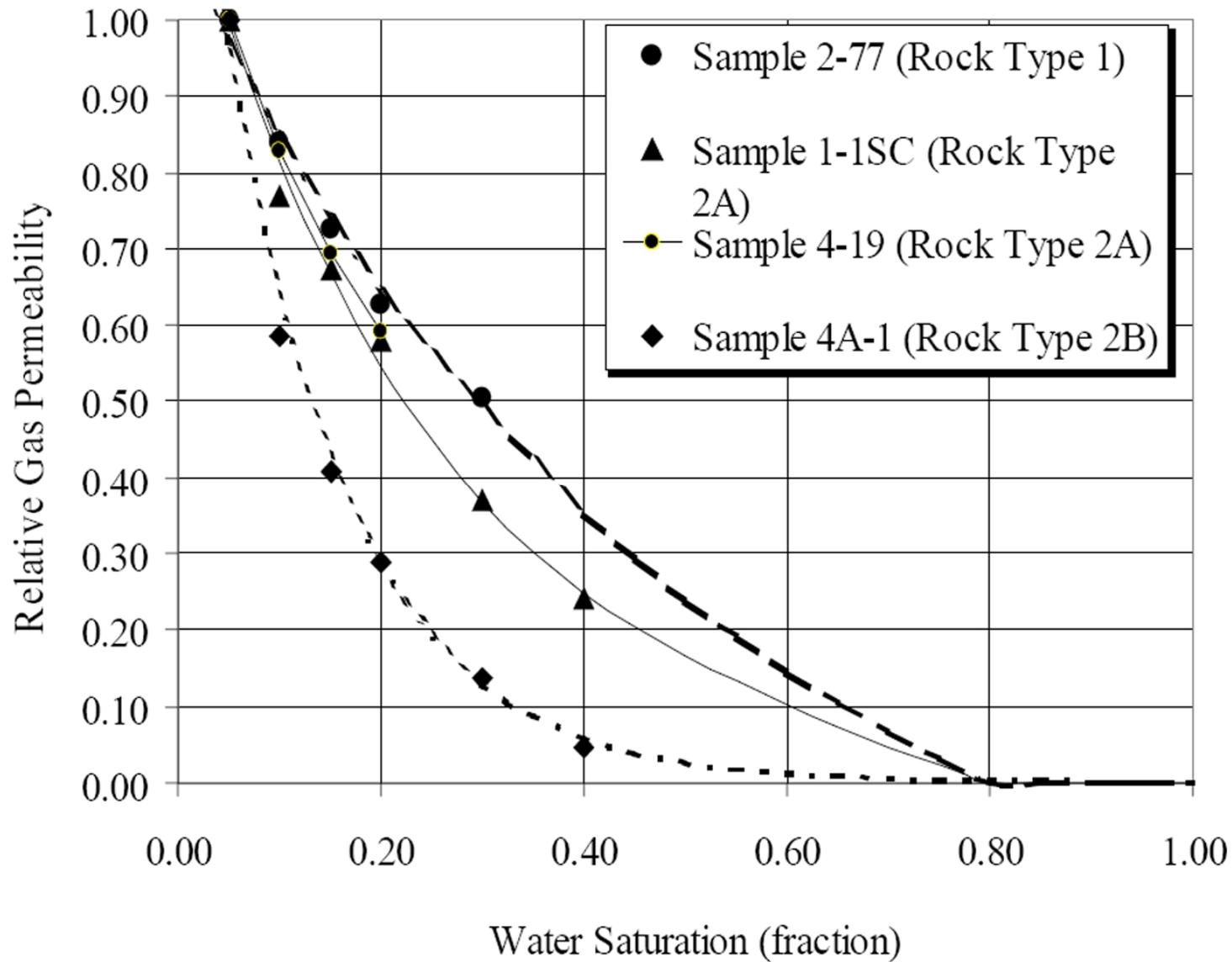
Figure 8. Relative permeability curves for hydraulic rock types 1, 2A and 2B. All curves were normalized to 5% initial water saturation based on the minimum water saturation measured in rock type 1.

Measurement Method	Primary Objective of Measurement
1) Routine helium porosity, unsteady-state permeability (horizontal P&P)	1) Provide a reservoir storage and flow capacity profile, rock type identification
2) Dean Stark fluid extraction from oil-based core	2) Describe the initial water saturation (Swi) conditions and profile; determine irreducible Sw
3) Slab core, polish slab face, and photo core using reflected white light and ultra violet light source	3) Describe sedimentary structures for genetic units, sequence, and depositional environment, observe mud invasion front as an early indicator of permeability.
4) Stressed dependent P&P	4) Describe the in-situ P&P, and Sw properties and observe the loss of P&P through a simulated depletion history.
5) X,Y,Z oriented P&P	5) Fully describe the permeability tensor and associated anisotropy.
6) Thin section photo micrographs, epifluoresence	6) Point counts for composition, grain size, sorting, pore distribution, paragenetic description, and petrographic rock typing
7) Stressed thin section photo micrographs, epifluoresence	7) Describe occurrence of in-situ micro-cracks
8) Xray diffraction (XRD), Fourier transform infrared spectroscopy (FTIR)	8) Relative abundance mineral presence and abundance.
9) Scanning electron microscopic surveys (SEM)	9) Describe pore geometry, clay type and habitat, micro-crack morphology
10) High pressure mercury, capillary injection (MICP)	10) Describe pore throat aperture, porosity, permeability, hydraulic rock type, irreducible Sw, seal capacity, and interpreted for hydrocarbon column height, and Sw profiles.
11) Electrical properties; Fr vs. porosity, Ri vs Sw, Co/Cw	11) Describe the the Archie parameters used for estimating Sw, correct "m" and "n" for excess conductance to "m*" and "n*".
12) Compression tests; unconfined compressive strength, hydrostatic, triaxial, Brazilian, uniaxial-depletion stress path	12) Describe the elastic moduli (Young's and Poisson's Ratio), strength envelope of each rock type, grain, bulk, and pore volume compressibility and the critical drawdown pressure at which rock failure occurs.
13) Regained permeability	13) Describe the rock-fluid interaction of various fluid types and the associated loss of permeability
14) Incremental phase trap, relative permeability	14) Describe the permeability of gas to flow under partial saturation conditions for each hydraulic rock type. Used in combination with the stressed dependent absolute permeability to describe effective permeability.
15) Commutation and fluid inclusion micro-thermometry	15) Determine the formation water salinity

Table 1. Typical core analysis: Methods for Bossier Sand description.

Hydraulic Rock Type	Absolute Permeability (mD) @ 800 psi	Pore Throat Radius, μ	Initial Water Saturation @ 1000' HAFW, %
1	$k_a > 0.5$	> 0.6	5 - 15
2A	$0.5 > k_a > 0.05$	$0.6 > r > 0.18$	10 - 30
2B	$0.05 > k_a > 0.015$	$0.18 > r > 0.10$	25 - 40
3A	$0.015 > k_a > 0.003$	$0.10 > r > 0.05$	35 - 45
3B	$0.003 > k_a > 0.00013$	$0.05 > r > 0.01$	40 - 55
4	$k_a < 0.00013$	$r > 0.01$	> 55

Table 2. Bossier Sand hydraulic rock type physical range of attributes.

Reservoir Description Program to Quantify WaterSaturation

To verify the low water saturations measured from the core plugs, we initiated a rigorous evaluation and validation program composed of three methods:

- Core-Based Measurements: direct water saturation measurements from Dean Stark extraction of core plugs;
- Log-Based Computations: computed vertical distribution of water saturation from well log response in three cored wells using measured Archie parameters (1950);
- Capillary-Equilibrium-Based Computations: assuming capillary equilibrium, computed vertical distribution of water saturation using geological structure.

Core-Based Water Saturation Measurements

We obtained more than 1000 ft of whole core from four wells in the Mimms Creek and Dew fields. To minimize invasion effects and preserve connate water saturation, we used an oil-base mud system. Properties of the oil-base mud included very low fluid loss as well as low surfactant energy. For most rock types, we consistently observed a mud invasion rind less than one inch in a four-inch diameter whole core, thus insuring accurate "preserved-state" water saturation measurements. Figure 9 illustrates a slightly larger invasion profile in one of the most permeable rocks (i.e., hydraulic rock type 1). Note, however, we still observe an undisturbed portion of the core.

Water saturation was measured directly with the Dean Stark solvent extraction process using toluene as the solvent. On the basis of more than 500 plugs, we observed water saturations ranging from as low as 5% in the best reservoir rock to more than 60% in the poor quality or non-reservoir rock.

Log-Based Water Saturation Calculations

We also computed the vertical distribution of water saturation in the same wells from which the core was obtained. The best match between core-based and log-based water saturation was obtained with the Modified Simandoux (1963) shaly sand model. Shale volume was estimated from the gamma ray response and porosity cross-plot techniques, while effective porosity was computed from a neutron-density cross-plot corrected for shale and gas effects.

Application of the Modified Simandoux (1963) model also requires estimates of the Archie (1950) saturation exponent, n, and the cementation exponent, m. These parameters were measured in the laboratory using both two-and four-electrode resistivity devices. Core samples were saturated with a 220,000 ppm brine, and all measurements were made at initial reservoir conditions; i.e., 3500 psia net stress and temperature of 300^oF. Results from both two- and four-electrode devices were in close agreement. The average values of m and n were 2.15 and 1.85, respectively. We also measured excess conductance using the Co/Cw method. Average corrected values of m* and n* were 2.2 and 1.87, respectively. The effect is minimized by the highly saline connate water.

The final component required to compute connate water saturation is water resistivity, Rw, at reservoir conditions. Unfortunately, direct sampling and testing of the formation water is impractical in the Bossier sands in the Mimms Creek and Dew fields. Low permeability and the associated relative permeability curves suggest a mobile water phase is improbable. Initial water production is mostly fracturing fluids from the stimulation treatment, while water produced following fracture clean-up is probably condensed water of vaporization. This observation is based upon the relatively low salinities observed in the produced water. Consequently, we used commutation analysis and fluid inclusion micro-thermometry to estimate connate water salinity from core samples.

Commutation or residual salt analysis is a process that extracts or leaches connate water and the associated salts from preserved core samples using ultra-pure, deionized water. Salt concentration and composition in the leachate are measured using an atomic absorption or mass spectrometer technique, while salinity is estimated from material balance calculations. Salinity measurements in the Bossier sands ranged from 200,000 to 230,000 ppm. Fluid inclusion micro-thermometry (FIT) uses thin sections from core samples to measure the temperature at which fluid inclusions melt. This melting temperature is directly related to the connate water salinity. Results from the FIT analysis ranged from 180,000 to 240,000 ppm, which is consistent with results from the commutation analysis. These results indicate the water resistivity ranges from 0.012 to 0.015 ohm-m at reservoir conditions.

In general, results from the log-based analysis agreed with water saturation estimates from the core measurements in the reservoir rock; however, some discrepancies were observed in the non-reservoir rock. An example of the match is illustrated in Figure 10.

Capillary-Equilibrium-Based Water Saturation Calculations

As we noted above, we also attempted to compute a vertical distribution of water saturation from capillary pressure characteristics to verify the apparent unusually low water saturations from the core and logs. We converted capillary pressures to height above free water and plotted them against water saturation. Our current understanding of the Bossier Sand geology in the Mimms Creek and Dew fields indicates the sands were deposited on a low-relief shelf/slope topography and appear to be laterally discontinuous. Under these conditions, the total relief is about 200 ft. Using this total column height, the computed range of irreducible water saturation is 35% to 100% for the reservoir rocks. This range, which is illustrated in Figure 11 as the dashed horizontal line, is significantly greater than the core-based measurements and log-based calculations, which ranged from 5% to 50% for the same reservoir-quality rocks.

Because of these discrepancies, our next step was to determine the column height required to match the range of water saturations determined from core and log analyses. Our calculations indicate an average total column height of 1000 ft is required to generate irreducible water saturations from 5% to 50% for rock types 1 through 3A, respectively. As shown by a solid horizontal line in Figure 11, this is consistent with the average seal capacity of the sealing facies. The capillary seal facies have a seal capacity ranging from 700 ft to 2000 ft and an average capacity of 1000 ft at a displacement saturation of 7.5%. This average seal capacity represents the upper threshold of column height for sands having 1000 ft of total relief. Current depositional and geological models of the Mimms Creek and Dew fields do not, however, support a 1000-ft column height.

Sub-capillary-Equilibrium Water Saturation Concept

In summary, vertical distributions of core-derived measurements and log-derived calculations of water saturation cannot be matched with estimates from capillary pressure characteristics unless we make unrealistic assumptions about sand geology and structure, particularly column height. This observation suggests the vertical distribution of water saturation in the Bossier sands may not be in capillary equilibrium. In fact, measured water saturation is much lower than that which would be predicted by capillarity; i.e., a sub-capillary-equilibrium or sub-irreducible water saturation condition. We also observed an abnormally high capillary pressure profile associated with the low water saturations. Although not common in the petroleum industry, this phenomenon has been observed and documented in basin-centered gas systems (Swarbrick and Osborne, 1998; Law, 1984a, b; 1994; Law and Dickinson, 1985; Masters, 1979, 1984; Ryder et al., 1996; Nuccio et al., 1992; Matinsen, 1994; Spencer, 1987; Meissner, 1987).
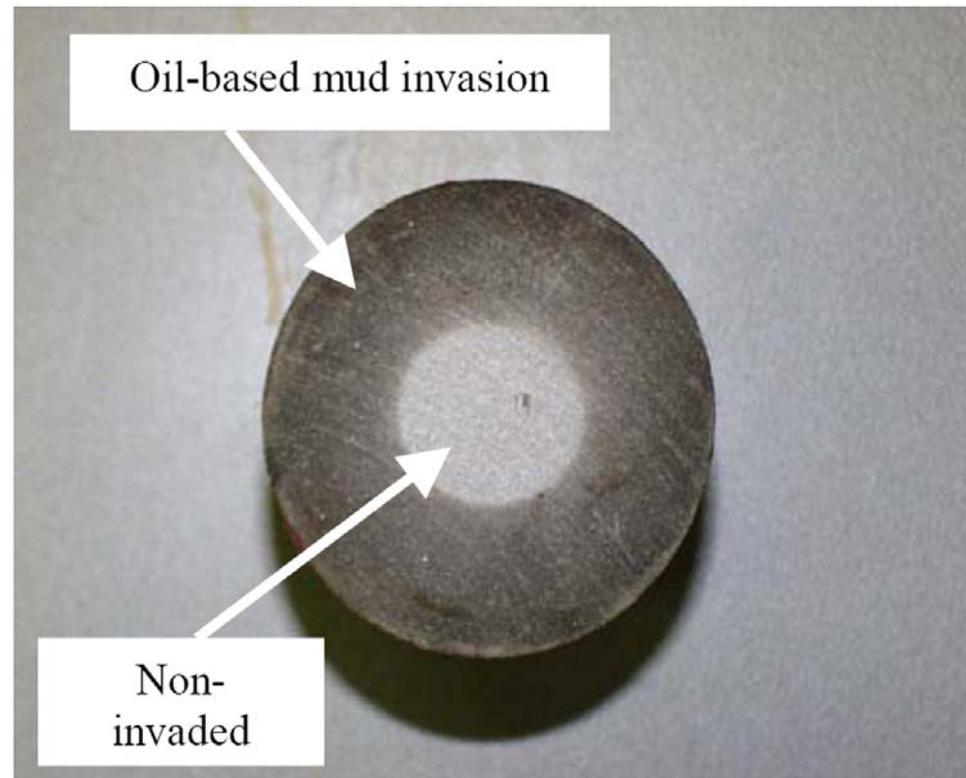
Figure 9. Photograph of a whole core section illustrating oil-based mud invasion profile in one of the most permeable rocks (i.e., hydraulic rock type 1). Note, however, we still observe an undisturbed portion of the core.
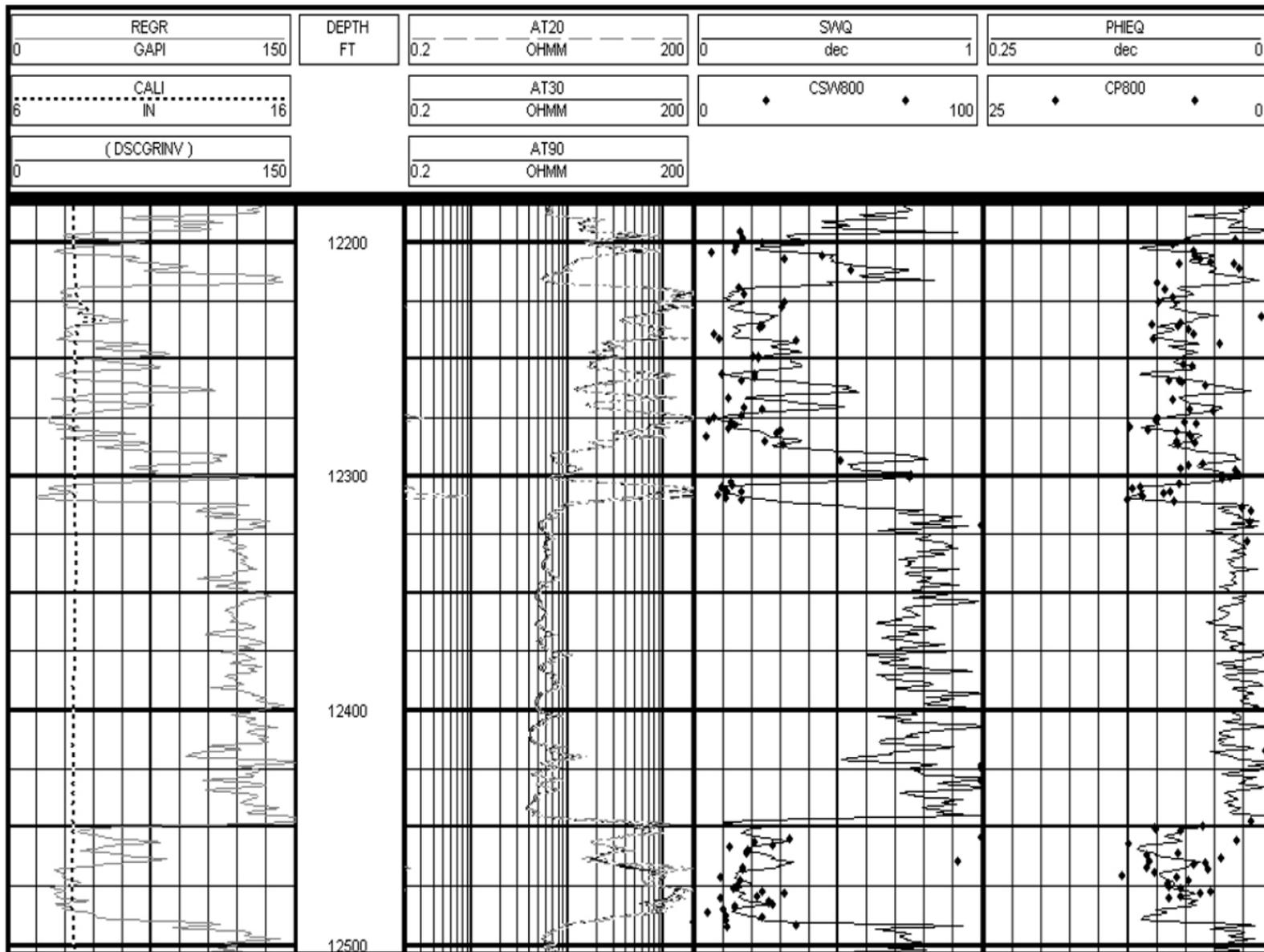
Figure 10. Log profile of gamma ray (track 1), resistivity (track 2), water saturation (track 3), and porosity (track 4). The discrete points represent the measured water saturation and porosity from the core. Note that there is close agreement between the core and log values for both water saturation and porosity.
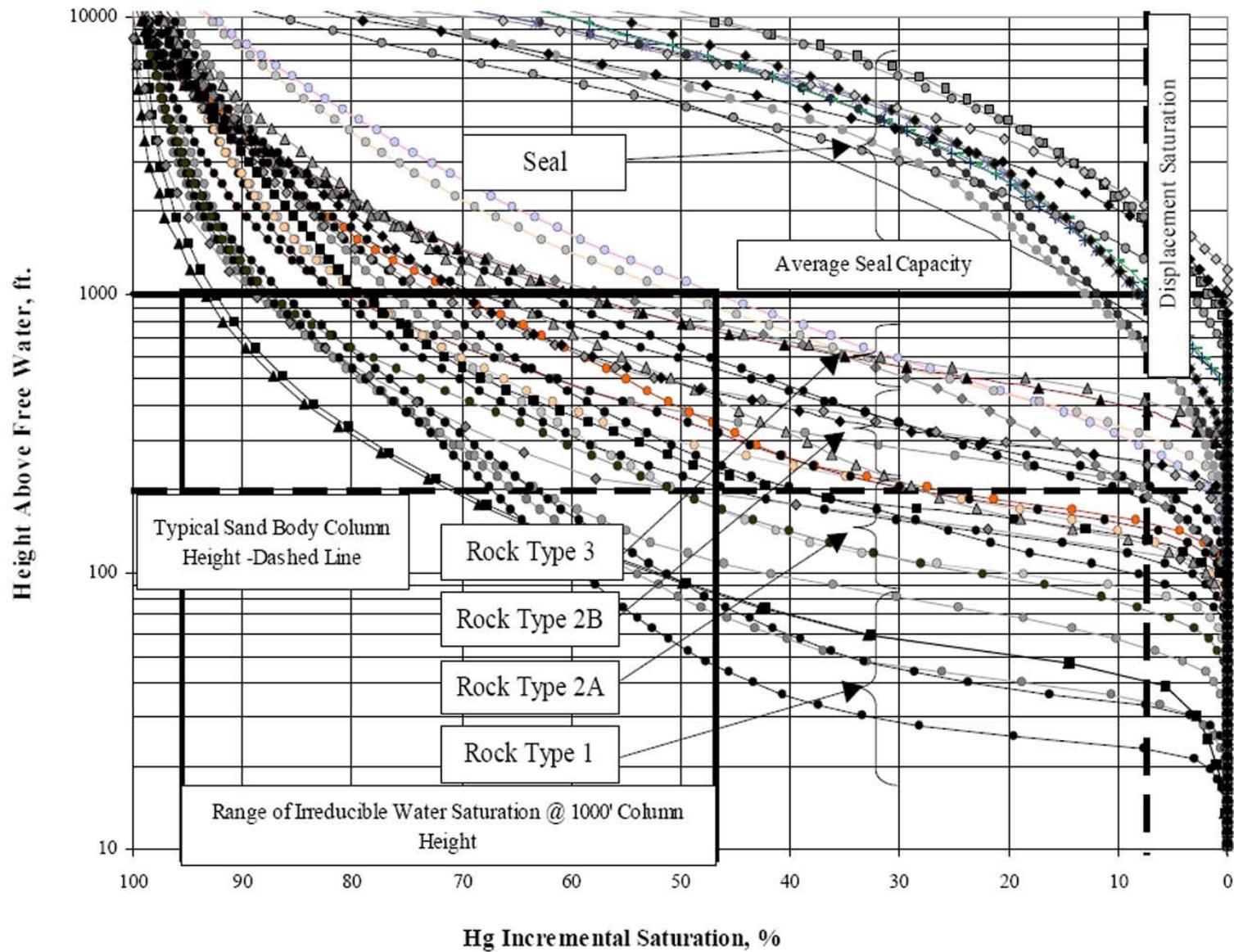
Figure 11. High pressure, mercury injection capillary pressure data converted to height above free water level. Note that the range of initial water saturation at 200 ft of column height is 30%-100%. It takes 1000 ft-2000 ft of column height to have water saturation in the measured range of 5%-40%.

Possible Mechanisms for Sub-Capillary-EquilibriumWater Saturation Phenomenon

In this section, we present a hypothesis to explain the physical mechanisms and conditions that could cause the development of a sub-capillary-equilibrium, water saturation distribution. We also present a geological process model under which this phenomenon would most likely occur. Our model is discussed as part of a total petroleum systems genesis but within the context of a basin-centered gas accumulation. Attributes of basin-centered gas systems are summarized in Table 3. Note that the Bossier sands and shales exhibit most of the properties listed in Table 3.

Elements of our Petroleum System Process Model are presented in Figure 12. These elements - i.e., source rock, reservoir rock, and reservoir seals - are very similar to conventional oil and gas systems. The reservoir rock is most often deposited as hydraulically isolated or disconnected sands interbedded with organic-rich marine shales. These sand-shale sequences usually occur as vertically stacked but isolated sands. As the sand-shale systems are buried by overlying sediments, the sands are buried deeper and exposed to higher pressures and temperatures. Continued burial and exposure to extreme environmental conditions causes the organic material to decay and generate hydrocarbons. Depending not only on the type and quantity of organic material but also the environmental conditions, organic diagenesis occurs in several discrete stages, resulting in generation of both liquid and gas hydrocarbons. If the shales are exposed to sufficiently high pressures and temperatures associated with the gas generation window, all hydrocarbons will be in the gas phase.

During all stages of shale diagenesis, hydrocarbons are frequently expelled from the shales and migrate into reservoir rock. If an adequate sealing system exists, then the hydrocarbons will be trapped in the reservoir rock. Sands in our model are isolated and interbedded with the shale; so shales most often act both as seals and local hydrocarbon sources. Continued hydrocarbon migration into the reservoir causes an increase in pore pressure until the shale seal capacity is exceeded, causing hydrocarbons to be expelled. Hydrocarbon expulsion continues until the reservoir pore pressure equilibrates with the shale seal capacity. At this point the shale heals and re-seals. As long as hydrocarbons are generated, the process becomes cyclical. We have given the cyclical process the acronym GENPERR (hydrocarbon generation, pressurizing, expelling, re-sealing, and recharging). This cyclical process explaining the petroleum system genesis has been documented by others (Swarbrick and Osborne, 1998; Law, 1984a, b; 1994; Law and Dickinson, 1985; Spencer, 1987; Meissner, 1987).

The critical element in our model is a mechanism to remove connate water effectively and transport the water up the vertical section. It has been recognized that several mechanisms can remove connate water from reservoir rock Meissner, 1987). None of these mechanisms alone, however, has the potential for removing large connate water volumes and establishing a sub-capillary-equilibrium, water saturation distribution. Most shales, even those with natural fractures, have a very low effective permeability to water. In addition, liquid water displacement by hydrocarbon gas is not a very effective mechanism for removing the water.

Consequently, we have identified another mechanism for removing connate water. We believe the key element required to remove water effectively is the process of vaporizing connate water into the gas phase. Laboratory data suggests that, at temperatures exceeding $280^{o}F$ to $300^{o}F$, significant volumes of water vapor may be dissolved in the hydrocarbon gas (McCain, 1990). Furthermore, the solubility of water vapor in gas is enhanced when non-hydrocarbon gases, such as CO_2 and H_2S, are present. We believe that most of the connate water displaced from the Bossier sands is in the form of

water vapor dissolved in the hydrocarbon gas. Gas generated and expelled from the shales is dry (i.e., initially no dissolved water vapor). As long as hydrocarbon gases continue to migrate into the reservoir, we have a mechanism to continuously vaporize and effectively remove connate water. In addition, the effective shale permeability to gas is much greater than that for water, thus allowing gas to flow more readily.

The final element required to explain a sub-capillary-equilibrium water saturation distribution is related to the hydrocarbon generation potential of the shales. For very organic-rich shales, hydrocarbon generation and migration may continue for thousands of years. Furthermore, if hydrocarbon migration into the reservoir is still ongoing and if the migration rate exceeds the rate at which hydrocarbons are expelled, then the reservoir conditions will be dynamic (albeit at very slow rates) rather than static. In addition, this dynamic condition should be manifested by varying degrees of abnormally high pressure gradients. Under normal conditions, a vertical distribution of water saturation in capillary equilibrium (i.e., static conditions) suggests surface wetting or adhesion forces are exactly balanced by gravitational forces. If, however, we have an external source of energy (i.e., influx of gas from source rock), then the vertical water saturation distribution cannot be in capillary equilibrium and we would not expect to encounter static conditions.
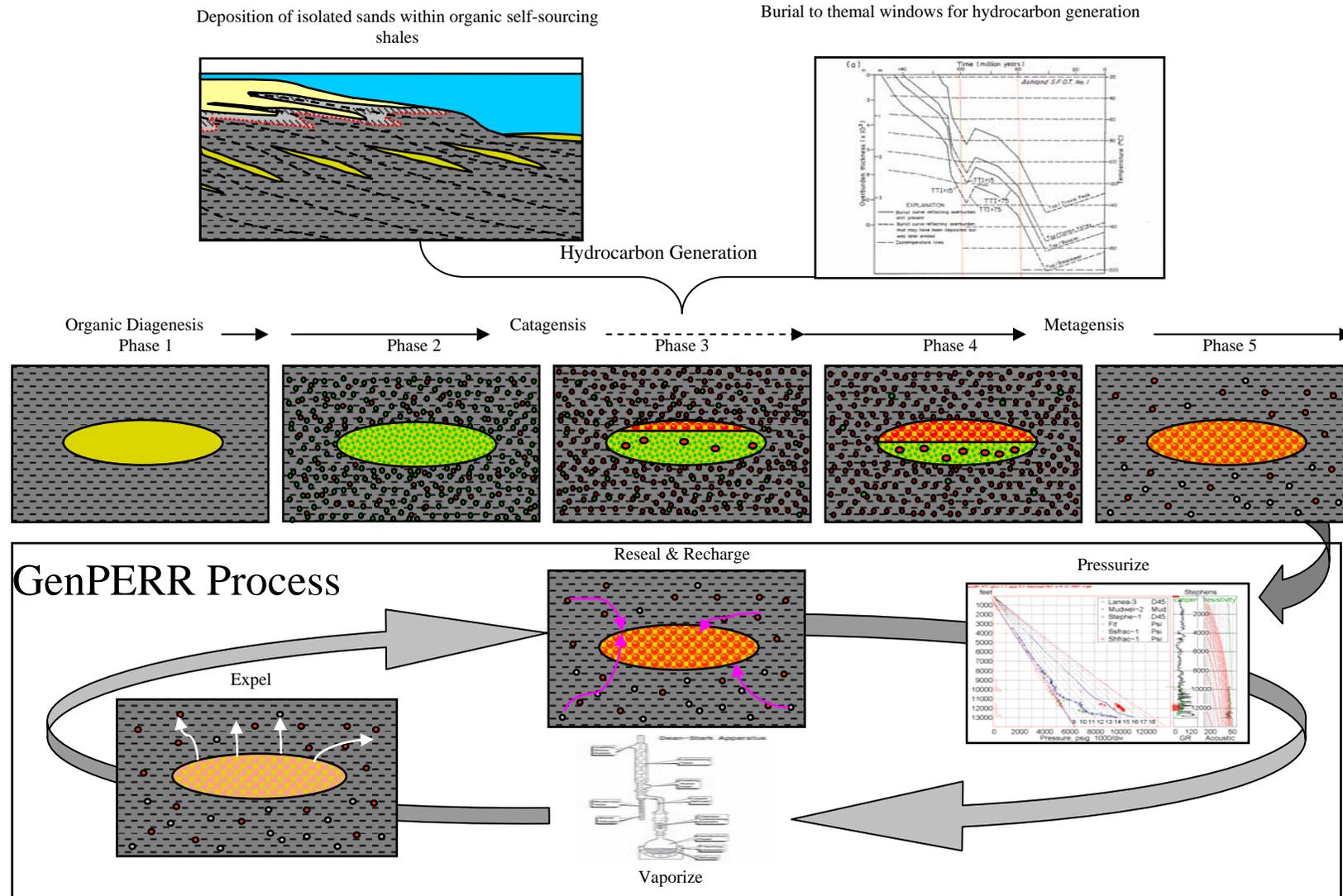
Figure 12. Elements of our Petroleum System Process Model: 1) Deposition of hydraulically isolated and low relief sands bodies onto organic rich, self-sourcing shale facies; 2) Burial of sand and increase in temperature and pressure; 3) Hydrocarbon generation via organic diagensis; 4) Local hydrocarbon migration into isolated sand bodies; 5) In-situ hydrocarbon catagenesis and metagenesis causing a build-up of pressure from the fluid volume exchange and removal of all but the irreducible pore waters; 6) Cyclic process of: a) pressurizing the isolated sand bodies, b) vaporizing the irreducible pore fluids, c) leaking due to seal breach by the abnormal pressure, d) resealing of the shale facies once the pressure has decreased below the seal pressure, e) recharging by interbedded organic shales that continue to generate hydrocarbons at a greater rate than they can be diffused.

Attribute Description
1) Geologic properties
Cretaceous Age (Masters, 1979, 1984)
Reservoirs may be single, isolated sand bodies or vertically stacked sands several 1000 feet thick (Law, 1984a, b, 1995; Law and Dickinson, 1985)
Structure and stratigraphy play a secondary role in the hydrocarbon accumulation (Law, 1984a, b, 1995; Law and Dickinson, 1985; Masters,
1979, 1984; Nuccio et al., 1996)
Top of BCGS as defined by top of abnormal pressure (TAG) cut across both structure and stratigraphy (Masters, 1979, 1984)
2) Shale characteristics and hydrocarbon generation potential
Local interbedded source rock (Nuccio et al., 1996)
Vitrinite > 1.1 (Ryder et al., 1996)
Top of BCGS > 0.7% Ro (Law, 1984a, b, Law and Dickinson, 1985)
Gas migration distance is short (Law, 1984a, b, Law and Dickinson, 1985)
Gas of thermal origin (Law, 1984a, b, 1995; Law and Dickinson, 1985; Masters, 1979, 1984)
Regionally pervasive gas accumulations, gas prone source rock (Law, 1984a, b, 1995; Law and Dickinson, 1985; Masters,
1979, 1984)
3) Abnormal pressure and temperature gradients
Primary pressure mechanism is hydrocarbon generation (Law, 1984a, b, 1995; Law and Dickinson, 1985)
Abnormally pressured gas accumulations (under and over pressure) (Law, 1984a, b, 1995; Law and Dickinson, 1985; Masters, 1979, 1984; Ryder et al., 1996)
Formation temperatures >150F (Ryder et al., 1996)
4) Rock and fluid properties
High formation water salinity; 200k - 300k TDS (Ryder et al., 1996)
Low permeability, typically < 1 mD (Law, 1984a, b, 1995; Law and Dickinson, 1985; Masters, 1979, 1984; Ryder et al., 1996)
Water most often present as irreducible (non-mobile) water (Law, 1984a, b, 1995; Law and Dickinson, 1985; Ryder et al., 1996)
Variable temporal seal integrity (Law, 1984a, b, 1995; Law and Dickinson, 1985)
Porosity less than 13% (Law, 1984a, b, 1995; Law and Dickinson, 1985; Ryder et al., 1996)
5) Production properties
Average water yield (beyond load water) 1 - 20 BW / MMSCF gas (Ryder et al., 1996)
Fracture stimulation required for commercial production (Masters, 1979, 1984)
Gas accumulations are down dip from normally pressured, water bearing reservoirs (Masters, 1979, 1984; Nuccio et al., 1992)
Gas accumulations do not have down dip water contacts (Law, 1984a, b, 1995; Law and Dickinson, 1985; Masters, 1979, 1984)
Large in-place hydrocarbon volume (Nuccio et al., 1996)
Low recovery factors (Nuccio et al., 1996)

Table 3. Common attributes of basin centered gas systems (BCGS).

Summary and Conclusions

We have documented an apparent sub-capillary-equilibrium water saturation distribution in the Bossier sands in the Mimms Creek and Dew fields, Freestone County, Texas. Our observations are based on consistent measurements and calculations from several different techniques and data sources. We have also postulated that the Mimms Creek and Dew fields may be part of a basin-centered gas system, and the mechanisms responsible for that system may have contributed to the unusually low water saturation distribution. We also believe that the Bossier sands in the Mimms Creek and Dew fields are not in capillary equilibrium. Finally, we have identified and provided evidence that water vaporization and dissolution in the hydrocarbon gas may be an effective mechanism for removing and transporting connate water up the vertical column.

Acknowledgments

References

Archie, G.E., 1950, Introduction to petrophysics of reservoir rocks: AAPG Bulletin, v.34, p.943-961.

Espitalie, J., Deroo, G., and Marquis, F., 1985, La pyrolyse Rock-Eval et ses applications: Rev. Inst. Fr. Pet. 40, p. 563579, p. 755-784, Rev. Inst. Fr. Pet. 41, p. 73-89.

Finkbeiner, T., Zoback, M., Flemmings,.P., and Stump, B., 2001, Stress, pore pressure, and dynamically constrained hydrocarbon columns in the South Eugene Island 330, northern Gulf of Mexico: AAPG Bulletin, v.85, no.6 (June 2001), p. 1007-1031.

Folk, R.L., 1974, Petrology of Sedimentary Rocks: Hemphill Publishing Co., Austin, Texas, 78703.

Gunter, G.W., et al., 1997, Early determination of reservoir flow units using an integrated petrophysical model: Paper SPE 38679 presented at the 1997 SPE Annual Technical Conference and Exhibition, San Antonio, TX, October 5-8.

Hunt, J.M., 1990, Generation and migration of petroleum from abnormally pressured fluid compartments: AAPG Bulletin, v. 74, no.1 (January 1990), p.1-12.

Law, B. E., 1984a, Relationships of source rocks, thermal maturity, and overpressuring to gas generation and occurrence in low-permeability Upper Cretaceous and lower Tertiary rocks, Greater Green River Basin, Wyoming, Colorado, and Utah, *in* Woodward, J., Meissner, F.F., and Clayton, J.L., eds., Hydrocarbon source rocks of the greater Rocky Mountain region: Rocky Mountain Association of Geologists, p. 469-490.

Law, B.E., 1984b, ed., Geological characteristics of low-permeability Upper Cretaceous and Lower Tertiary rocks in the Pinedale anticline area, Sublette County, Wyoming: U.S. Geological Survey Open-File Report 84-753, 107 p.

Law, B.E., 1995, Columbia Basin-basin-centered gas play (0503), *in* Tennyson, M.E., Eastern OregonWashington Province (005), *in* Gautier, D.L., Dolton, G.L., Masters, J.A., 1979, Deep basin gas trap, western Canada: AAPG Bulletin, v. 63, p.152-181.

Law, B.E., and Dickinson, W.W., 1985, A conceptual model for the origin of abnormally pressured gas accumulations in low-permeability reservoirs: AAPG Bulletin, v.69, p.1295-1304.

Leverett, M.C., 1941, Capillary behavior in porous sands, Trans. AIME, 1941.

Gunter, G., et. al., 1999, Saturation modeling at the well log scale using petrophysical rock types and a classic non-resistivity based method: 40th Annual SPWL Symposium, Paper ZZ.

Masters, J.A., 1984, ed., Elmworth - Case study of a deep basin gas field: AAPG Memoir 38, 316 p.

Matinsen, R.S, 1994, Summary of published literature on anomalous pressures: implications for the study of pressure compartments, *in* Ortoleva, P.J. ed., AAPG Memoir 61, 1994.

McCain, W.D., 1990, The Properties of Petroleum Fluids, 2nd Edition: Penwell Publishing Company, 548 p.

Meissner, F.F, 1987, Mechanisms and patterns of gas generation/storage/explusion-migration/accumulation associated with coals measures in the Green River and San Juan Basins, Rocky Mountain. Region, USA, *in* Dolgigez, B., ed.,Migration of hydrocarbons in sedimentary basins:, 2nd IFP Exploration Research Conference, Carcias, France, June 15-19, 1987, Editions Technip. Paris, p. 79-112.

Montgomery, S., 2000, East Texas Basin Bossier gas play in petroleum frontiers, Anderson, J., ed.: IHS Energy Group, Englewood CO (2000), p. 1-60.

Negabahn, S., et.al., 2000, An improved empirical approach for prediction of formation water saturation and free water level for uni-modal pore systems: SPE 63282, 2000 SPE Annual Technical Conference and Exhibit, Dallas, TX., October 1-4, 2000.

Newsham, K.E., and Rushing J.A., 2001, An integrated work-flow model to characterize unconventional gas resources—Part I: Geological assessment and petrophysical evaluation: Paper SPE 71351 presented at the 2001 SPE Annual Technical Conference and Exhibition, New Orleans, LA, Oct. 1-3.

Nuccio, V.F., Schmoker, J.W., and Fouch, T.D., 1992, Thermal maturity, porosity, and lithofacies relationships applied to gas generation and production in Cretaceous and Tertiary low-permeability (tight) sandstones, Uinta Basin, Utah., *in* Fouch, T.D., Nuccio, V.F., and Chidsey, T.C., Jr., eds., Hydrocarbon and mineral resources of the Uinta Basin, Utah and Colorado: Utah Geological Association Guidebook 20, p. 77-94.

Perrizela,P. , 2002, OMNI Core description reports, McAdams A7, Henderson 6, and Burgher D7.

Pittman, E.D., 1992, Relationship of porosity and permeability to various parameters derived from mercury injection-capillary pressure curves for sandstone: AAPG, v. 76, no. 2 (February 1992), p. 191-198.

Prouty, J.L., 2001, Tight gas in the spotlight," *in* GasTIPS, Gavin, J.J. and Lang, K.R., eds., Gas Technology Institute, v. 7, no. 2, Chicago, IL (2001), p.. 4-10.

Ryder, R.T., SanFilipo, J.R., Hettinger, R.D., Keighin, C.W., Law, B.E., Nuccio, V.F., Perry, W.J., and Wandrey, C.J., 1996, Continuous-type (basin-centered) gas accumulation in the Lower Silurian "Clinton" sands, Medina Group, and Tuscarora Sandstone in the Appalachian Basin: AAPG Bulletin, v. 80, p. 1531.

Simandoux, P.,1963, Measures dielectrique en milieux poreux, application a measure de saturation en eau, etude des massifs argileaux: Revue de l'institut Francais du Petrole, Supplement issue, 1963, p. 193-215.

Spencer, C.W., 1987, Hydrocarbon generation as a mechanism for overpressuring in the Rocky Mountain region, AAPG Bulletin v. 71, no. 4 (April 1987), p. 368-388.

Swanson, B.F., 1979, A simple correlation between permeabilities and mercury capillary pressure: Paper SPE 8234, 54th Annual Technical Conference and Exhibition, Las Vegas, NV, September 23-26, 1979.

Swarbrick, R.E., and Osborne, M.J., 1998, Mechanisms that generate abnormal pressures: an overview, *in* Law, B.E., Uimishek, G.F., and Slavin, V.I., eds., Abnormal pressures in hydrocarbon environments: AAPG Memoir 70, p. 13-34.

Takahashi, K.1., and Varnes, K., eds., 1995 National assessment in the United States of oil and gas resources: Results, methodology, and supporting data: U.S. Geological Survey Data Series 30.

Thompson, A.H., et al., 1987, Estimation of absolute permeability from capillary pressure measurements: Paper SPE 16794 presented at the 1987 SPE Annual Technical Conference and Exhibition, Dallas, Texas, September 27-30.

Washburn, E.W., 1921, Note on a method of determining the distribution of pore sizes in a porous material: Proceedings of the National Academy of Science, v. 7, p.115-116.